

# Air Turborocket/Vehicle Performance Comparison

Kirk Christensen\*

KC Consulting Engineering, Rolla, Missouri 65401

The air turborocket (ATR) possesses design, performance, and operation characteristics of the turbojet, ramjet, and rocket in a single air-breathing propulsion system. The basic design tradeoff of ATR design is specific thrust and specific impulse. There are many possible variations to this basic cycle, but this research has concentrated on the solid-fuel gas-generator-driven ATR. Because overall vehicle performance is more important than engine-only operation, the evaluation of any propulsion system must be done at the vehicle level. The results of this study show that an 807-lbm solid-rocket-motor- (SRM-) powered vehicle achieves a range of 28.2 miles in 98.1 s. A 750-lbm ATR-powered vehicle attains a range of 49.8 miles in 192 s. A 525-lbm turbojet-powered vehicle will travel 49.6 miles in 290 s. This means that the ATR will provide nearly double the range of an SRM-powered vehicle with roughly double the flight time. Compared with the equal volume turbojet-powered vehicle, the ATR-powered vehicle achieves the same range in about two-thirds of the turbojet flight time with a 43% greater initial system mass.

## Nomenclature

$C_p$	= specific heat at constant pressure, Btu/lbm-R
$g_0$	= gravity constant, 32.174 lbf-ft/(lbf-s <sup>2</sup> )
$I_{sp}$	= specific impulse, lbf-s/lbm
$\gamma$	= ratio of specific heats
$\eta_{comb}$	= combustion efficiency
$\eta_{comp}$	= compressor efficiency
$\eta_{turb}$	= turbine efficiency
$\pi$	= pressure ratio

## Subscripts

air	= airflow
amb	= ambient conditions
comb	= combustor gas
comp	= compressor
exit	= nozzle exit plane
$t$	= total conditions
turb	= turbine drive gas

## Introduction

THE air turborocket (ATR) possesses design, performance, and operation characteristics of the turbojet, ramjet, and rocket engine in a single air-breathing propulsion system. It is illustrated schematically in Fig. 1. As the figure shows, the turbine drive gas is supplied from a gas generator that operates independently of the airflow through the engine. Thus, ATR turbine inlet temperature, unlike the turbojet, is not constrained by the vehicle flight condition. The ATR can generate net positive thrust from sea-level static conditions to Mach 5–6 flight conditions without a booster propulsion system. The ATR has an inherently higher maximum operating speed and altitude than a turbojet because 1) the compressor rather than the turbine is the temperature-limiting component of the ATR and 2) the gas temperature at the turbine inlet of the turbojet is normally higher than the air temperature at the compressor exit. The ATR compressor provides a higher combustor pressure than that available from ram pressure alone at any given flight condition. Because the minimum combustor pressure is a major influence on the maximum altitude at which stable combustion can be maintained, the maximum operating altitude of the ATR is inherently higher than that of a ramjet.

The solid-fuel gas-generator ATR is an ATR in which the propellant is stored as a solid grain in the gas generator. The gas generator provides the turbine drive gas for operation of the turbomachinery as well as providing fuel for combustion in the main combustor. Like a solid-rocket motor (SRM), a solid-fuel gas generator can be throttled, but is not easily shut down completely. The issue of solid-fuel gas-generator ATR throttling is addressed in more detail later.

Although there are many possible variations of the ATR cycle, this paper concentrates on the basic cycle represented in Fig. 1. Most of the test articles built to date in the U.S. have demonstrated operation and throttability of the ATR at static conditions.<sup>1–6</sup> However, vehicle performance parameters such as flight time and range are the criteria against which the ATR must be measured for comparison with other propulsion systems. Determining the range and flight time of ATR-powered vehicles is the major goal of this research.

## Specific Impulse vs Specific Thrust

The basic tradeoff of the ATR design procedure is between specific thrust and  $I_{sp}$ .  $I_{sp}$ , the ratio of net engine thrust to propellant mass flow rate, is the most important propulsion system performance parameter. The essential goal of the ATR design procedure is to maximize  $I_{sp}$ , while meeting vehicle and/or engine size, weight, and cost constraints. Specific thrust on the other hand is an important indicator of air-breathing engine size. As specific thrust increases, the airflow for a given thrust level decreases. As airflow rate decreases, the required compressor and inlet size are also reduced. Combustor size is also reduced by a reduced airflow rate. Combustor size can also be reduced by increasing the compressor pressure ratio. A higher combustor pressure will require a smaller combustor for a given thrust. A higher compressor pressure ratio will also reduce compressor and inlet size because, for a fixed thrust level, a higher compressor pressure ratio generally requires a higher fuel/air ratio. As will be seen, a higher fuel/air ratio tends to increase specific thrust. Ultimately, engine size has a significant effect on vehicle performance because it affects the aerodynamic characteristics of the vehicle.

The relationship between specific thrust and  $I_{sp}$  can be seen in the following equations, which define the 1) fuel/air ratio of the ATR, 2)  $I_{sp}$  as a function of the fuel/air ratio, and 3) specific thrust as a function of the fuel/air ratio at design and off-design operating conditions.

Equation (1) is derived from a power balance between the compressor and turbine. The equation assumes first-law characterizations of both the compressor and turbine modified by an efficiency for each component. Note that the heating value of the fuel should not appear in this expression because the efficiency of power extraction from the turbine drive gas is not a function of the fuels'

Received 20 June 1998; revision received 21 December 1998; accepted for publication 4 January 1999. Copyright © 1999 by the American Institute of Aeronautics and Astronautics, Inc. All rights reserved.

\*President, 10954 Hanley Drive.

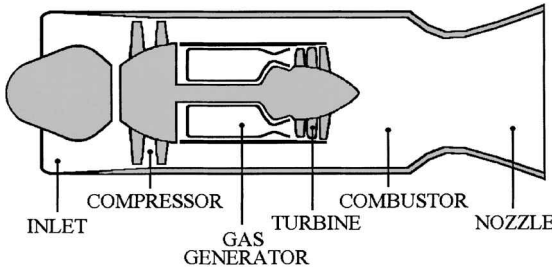


Fig. 1 ATR schematic.

heat-release potential when burned with air. The resulting expression is

$$\text{air/fuel} = \frac{T_{t\text{comp}} C_{p\text{air}} \left[ \pi_{\text{comp}}^{(\gamma_{\text{air}} - 1)/\gamma_{\text{air}}} - 1 \right]}{\eta_{\text{comp}} \eta_{\text{turb}} T_{t\text{turb}} C_{p\text{turb}} \left[ 1 - (1/\pi_{\text{turb}})^{(\gamma_{\text{turb}} - 1)/\gamma_{\text{turb}}} \right]} \quad (1)$$

This expression is valid for the basic ATR cycle, even if the turbine drive gas and airflow do not mix.

Related expressions for both specific thrust and  $I_{\text{sp}}$  can also be defined analytically in terms of the fuel/air ratio. In this way, turbomachinery characteristics such as compressor pressure ratio  $\eta_c$ , turbine pressure ratio, and  $\eta_t$  can be related to specific thrust and  $I_{\text{sp}}$ .

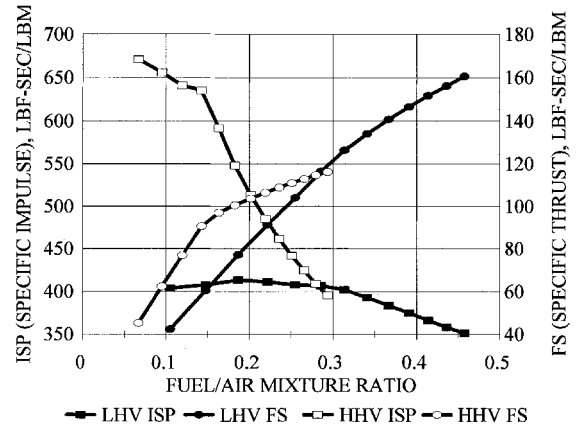
Equation (2) defines  $I_{\text{sp}}$  in terms of the fuel/air ratio:

$$I_{\text{sp}} = \frac{(\text{fuel/air}) + 1}{(\text{fuel/air})} \times \sqrt{\frac{2R\gamma_{\text{comb}}\eta_{\text{comb}}T_{\text{comb}}}{g_0(\gamma_{\text{comb}} - 1)MW_{\text{comb}}}} \left[ 1 - \left( \frac{P_{\text{exit}}}{P_{\text{comb}}} \right)^{(\gamma_{\text{comb}} - 1)/\gamma_{\text{comb}}} \right] + \frac{P_{\text{exit}} - P_{\text{amb}}}{\dot{m}_{\text{turb}}} A_{\text{exit}} - \frac{V_{\text{air}}}{(\text{fuel/air})g_0} \quad (2)$$

The first term in this equation is the  $I_{\text{sp}}$  that would result if the combustor gas expanded isentropically to the nozzle exit pressure without any pressure difference acting at the exit plane of the nozzle. The  $(\text{fuel/air} + 1)/\text{fuel/air}$  ratio factor appearing in this equation is very important. It is the ratio of total mass flow rate through the engine to the fuel mass flow rate. Although not readily apparent, analyses has shown that for almost all propellants, the increase in this factor, as the fuel/air ratio drops, is greater than the decrease in the main combustor gas temperature. Note that the equilibrium combustor gas temperature/main combustor gas temperature is multiplied by  $\eta_{\text{comb}}$  to define the predicted actual combustor gas temperature. The second term represents the increase (or decrease) in thrust due to any pressure difference acting over the nozzle exit area. The last term represents the thrust loss due to the momentum of the entering airstream, usually referred to as ram drag. This  $I_{\text{sp}}$  loss increases as the fuel/air ratio is reduced because this means a larger airflow for a given thrust level.

If all parameters in this equation except the fuel/air ratio are held constant, a plot of  $I_{\text{sp}}$  vs the fuel/air ratio shows that  $I_{\text{sp}}$  decreases, and specific thrust increases as the fuel/air ratio increases. Analyses performed by the author<sup>7</sup> show that this trend generally holds even for fuel-lean ATR combustors where a decreasing fuel/air ratio means a decreasing main combustor gas temperature. Thus, unlike rocket engines, ATR  $I_{\text{sp}}$  continues to increase as the fuel/air ratio decreases, even when the combustor operates significantly fuel-lean. In other words, the lower the ATR fuel/air ratio, the higher the theoretically possible  $I_{\text{sp}}$ . Rocket-engine  $I_{\text{sp}}$ , on the other hand, usually maximizes close to the stoichiometric fuel/oxidizer ratio.

Therefore, in general, any ATR component design change that reduces the fuel/air ratio will enable a higher  $I_{\text{sp}}$  and vice versa. This trend is limited by the effect of combustor pressure. Equation (2) shows that reduced combustor pressure will degrade  $I_{\text{sp}}$ . That is,

Fig. 2  $I_{\text{sp}}$  and specific thrust vs fuel/air mixture ratio.

when the compressor pressure ratio and resulting combustor pressure are low enough,  $I_{\text{sp}}$  will be reduced regardless of the fuel/air ratio.

Equation (3) for specific thrust as a function of the fuel/air ratio is easily derived from the  $I_{\text{sp}}$  expression. As before, the first two terms determine the specific thrust generated by isentropic expansion of the combustor gas from the main nozzle and the effect of the pressure difference acting at the nozzle exit plane. The last term is the specific thrust loss due to ram drag. This resulting equation is

$$\text{Specific Thrust} = \left( \frac{\text{fuel}}{\text{air}} + 1 \right) \times \sqrt{\frac{2R\gamma_{\text{comb}}\eta_{\text{comb}}T_{\text{comb}}}{g_0(\gamma_{\text{comb}} - 1)MW_{\text{comb}}}} \left[ 1 - \left( \frac{P_{\text{exit}}}{P_{\text{comb}}} \right)^{(\gamma_{\text{comb}} - 1)/\gamma_{\text{comb}}} \right] + \frac{(\text{fuel/air})}{\dot{m}_{\text{turb}}} (P_{\text{exit}} - P_{\text{amb}}) A_{\text{exit}} - \frac{V_{\text{air}}}{g_0} \quad (3)$$

As this equation shows, specific thrust increases with the fuel/air ratio.

The effect of the fuel/air ratio on both  $I_{\text{sp}}$  and specific thrust is illustrated in Fig. 2, which was generated using Eqs. (2) and (3). These results show the equilibrium main combustor gas temperature as a function of the fuel/air ratio for two solid grain formulations: 1) a higher heating value ( $\sim 11,000$  Btu/lbm) propellant and 2) a lower heating value (6000 Btu/lbm) propellant. This figure clearly shows the tradeoff between  $I_{\text{sp}}$  and specific thrust. For these results, turbine pressure ratio was held constant and compressor pressure ratio was varied. The higher heating value propellant provides superior  $I_{\text{sp}}$  and specific thrust at lower fuel/air ratio values. However, as the fuel/air ratio increases, the lower heating value propellant provides the superior  $I_{\text{sp}}$  and specific thrust. Each propellant has a feasible range of operating fuel/air ratio that is established by the 1) turbomachinery characteristics and 2) turbine drive gas properties associated with each propellant. These fuel/air ratio limits can be calculated using Eq. (1). A high turbine pressure ratio and low compressor pressure ratio promote a low fuel/air ratio. Conversely, a low turbine pressure ratio and high compressor pressure ratio promote a high fuel/air ratio. As the compressor pressure ratio is reduced or the turbine pressure ratio is increased, the fuel/air ratio will be reduced.

In both equations, and as illustrated in Fig. 2,  $I_{\text{sp}}$  and specific thrust are continuous functions of the fuel/air ratio, even though there is an inflection point in the curve when the combustor begins operating fuel-rich. As the fuel/air ratio increases beyond this point, the combustor gas temperature is reduced. However, the reduction in the main combustor gas temperature is generally less, on a percentage basis, than the increase in the  $(\text{fuel/air} + 1)/\text{fuel/air}$  ratio factor, which also drives  $I_{\text{sp}}$ . Thus,  $I_{\text{sp}}$  increases for a fuel-lean ATR even when the main combustor gas temperature drops.

## ATR Turbomachinery Design Considerations vs Cruise Mach

Preferred turbomachinery characteristics vary widely with the design cruise Mach. For low-speed missions, specific thrust can be lower because the inlet spillage drag is less at lower speeds for a fixed airflow rate. Because specific thrust may be traded for  $I_{sp}$ , a higher  $I_{sp}$  is possible. The goal is to maximize mission-average  $I_{sp}$  without violating the minimum allowable specific thrust anywhere during the flight.

For fuel-lean operation, a lower compressor pressure ratio will promote a higher  $I_{sp}$  and a lower specific thrust. This increases the size of the combustor and total combustor flow rate.

The lower limit on compressor pressure ratio is established when either 1) the combustor volume becomes excessive or 2) the combustor pressure is so low that it begins to degrade  $I_{sp}$ . A higher design point compressor pressure ratio also increases the potential throttle range. Vehicle envelope constraints may require an even smaller combustor size that will further increase the minimum acceptable specific thrust. In all cases,  $\eta_{comb}$  should be as high as possible because reduced  $\eta_{comb}$  reduces both specific thrust and  $I_{sp}$ .

In the case of the turbine, turbine pressure ratio should be as high as possible because this promotes high  $I_{sp}$  at the cost of reduced specific thrust. In general, the limiting factor on maximum turbine pressure ratio is the required turbine inlet pressure that is constrained by the maximum gas-generator pressure. Above this maximum pressure, the gas generator may become heavy enough to degrade vehicle performance. The effect of turbine pressure ratio on combustor volume is not as great as that of compressor pressure ratio. This conservative conclusion assumes there is no total pressure gain from the gas-generator flow into the combustor. That is, combustor pressure is assumed equal to the compressor exit pressure less any pressure losses between the compressor discharge and combustor plenum. The turbine exhaust gas is then assumed to expand as needed to match the static pressure in the combustor.

In the case of a high-speed mission, engine size becomes crucial because of inlet spillage drag. Both the frontal area and combustor volume should be reduced so as to produce the required thrust with adequate  $I_{sp}$ . Thus, increased compressor pressure ratio is nearly always required for high-speed ATR designs. Reducing the turbine pressure ratio will increase the fuel/air ratio, which will reduce the required airflow for a given thrust and thus reduce frontal area. However, this also degrades  $I_{sp}$ . An approach not recommended is to purposefully degrade  $\eta_{turb}$ , because this increases specific thrust but also reduces  $I_{sp}$  and increases the required turbine inlet pressure. Reducing turbine pressure ratio on the other hand reduces the required turbine inlet pressure.

## Heating Value

As noted previously, a heating value does not appear in the expression that defines the fuel/air ratio at which the ATR operates. However, a fuel heating value is useful for comparing turbojet fuels. In the case of the turbojet, combustion gas characteristics such as molecular weight and  $\gamma$  vary little because the combustor gas is mostly air. The turbojet combustor is usually operated fuel lean to limit the turbine inlet temperature. In this case, more thrust is available by afterburning downstream of the turbine. Thus, a very important turbojet propellant characteristic is a high heating value that minimizes the amount of fuel required to raise the combustor gas temperature to the maximum allowable value.

The heating value is a less important evaluation criteria for the ATR propellants, compared with the turbojet, because the ATR turbine-drive gas does not come from fuel/air combustion. Thus the turbine-drive gas molecular weight and  $\gamma$  cannot be taken as constants for the purposes of comparing ATR propellants. An engine-level comparison of ATR propellants must be made on the basis of  $I_{sp}$  and specific thrust, not on whether the main combustor is operating either fuel-rich or fuel-lean.

If a propellant has a high heating value, it means that the stoichiometric fuel/air ratio will be low. In effect, for a fixed airflow rate, less of the high heating value fuel is needed to achieve the same combustion gas temperature compared with a low heating value

propellant. However, high heating value propellants often generate a higher  $C_p$  gas. The higher the  $C_p$ , the lower the mass flow rate of the gas required to drive the turbine. Thus, both the fuel/air ratio and the stoichiometric fuel/air ratio will be relatively low. Conversely, for a low heating value propellant, the stoichiometric fuel/air ratio will generally be high. However, low heating value propellants often generate a relatively low  $C_p$  gas. The lower the  $C_p$ , the higher the mass flow rate of the gas required to drive the turbine. Thus, both fuel/air ratio and the stoichiometric fuel/air ratio will be relatively high. Therefore, the determination of fuel-rich or fuel-lean ATR operation is not possible from a consideration of heating value alone.

Two other ATR propellant considerations are noted here. First, the presence of hydrogen in the gas generator exhaust is often characteristic of high heating value propellants. Gaseous hydrogen has a very high  $C_p$ . In fact, the presence of hydrogen can be a major reason why the fuel/air ratio and the stoichiometric fuel/air ratio are both low when high heating value propellants are evaluated for use in the ATR. Second, for some propellants, the gas generator effluent gas may contain solid carbon (soot). The carbon increases the predicted heating value of the turbine drive gas when burned with air, but it does not expand in the turbine and thus does not increase the available turbine power. This increases the fuel flow required to drive the turbine and thus increases the fuel/air ratio above the value that would be obtained with complete extraction of work from the turbine drive gas.

In summary, a fuel-rich ATR with a superior  $I_{sp}$  and specific thrust is preferred over a stoichiometric or fuel-lean ATR design with inferior  $I_{sp}$  and specific thrust. Thus, ATR propellants should be compared on the basis of their  $I_{sp}$  and specific thrust potential instead of their heating value.

## Solid-Fuel Gas-Generator Throttling

Solid-fuel gas-generator throttling is accomplished by means of a gas-generator valve through which the exhaust gases flow from the solid-fuel gas-generator chamber. This valve determines the minimum area, or throat, through which the solid-fuel gas-generator exhaust gas flows before encountering the turbine nozzle throat area(s). Depending on the ratio of the chamber pressure and the pressure downstream of the gas-generator valve, the flow velocity through the valve throat will be sonic or subsonic. Sonic velocity corresponds to the maximum, or "choked," mass flow rate for the given valve setting. A subsonic flow velocity indicates a less-than-maximum mass flow rate for the given valve setting. The pressure ratio is generally high enough to cause sonic velocity through the gas-generator valve throat. Once this maximum flow rate is achieved, any reduction in downstream pressure will not affect the mass flow rate through the gas-generator valve. However, if the pressure downstream of the gas-generator valve is increased enough, the valve will "unchoke" and the flow through it will become subsonic. This flow rate can be further reduced by variations in either the solid-fuel gas-generator plenum pressure or pressure downstream of the gas-generator valve. The variation of the solid-fuel gas-generator mass flow rate with the gas-generator valve setting is enabled by the fact that the mass flow rate of a solid-fuel gas generator is physically generated by the burning of the solid grain propellant over a finite area inside the plenum, usually referred to as the "burning area." The rate at which the solid grain burns is a strong function of the solid-fuel gas-generator plenum pressure. For a fixed burning area, closing the gas-generator valve causes the plenum pressure to increase, whereas opening the gas-generator valve reduces the plenum pressure. The net effect of these characteristics is that the gas-generator valve is closed to increase the solid-fuel gas-generator mass flow rate and opened to reduce the solid-fuel gas-generator mass flow rate. Because the solid-fuel gas-generator exhaust gas drives the turbine, the thrust level of the ATR is controlled by the setting of the gas-generator valve. The mass flow rate through the turbine nozzle throats, which is the same as the solid-fuel gas-generator mass flow rate, can also be sonic or subsonic, again depending on the pressure ratio of the upstream to downstream pressures. In fact, it is the presence of these nozzle throat area(s) that establishes the lower limit for throttling

of the solid-fuel gas-generator ATR. Effectively, throttling of the solid-fuel gas-generator ATR is a two-throats-in-series problem in which both throats operate in a choked condition, with the first throat determining the mass flow rate. The lower throttling limit is reached when the gas-generator valve opens sufficiently so that flow through it becomes unchoked because of the reduced ratio of the upstream and downstream pressures. At this point, the turbine nozzle throats (fixed), which are usually still choked, now determine the gas-generator flow rate. Opening the gas-generator valve beyond this point has little effect on gas-generator flow rate, and therefore, on ATR operation. This lower throttling limit can be increased by designing into the ATR a large total pressure loss between the gas-generator valve and turbine nozzles. This is done by reducing the size of the gas-generator valve throat area relative to the turbine throat area. The greater the desired pressure drop, the greater this relative size difference will be. This assumes that the major portion of the total pressure drop is due to an equivalent normal shock between the gas-generator valve and turbine inlet. Depending on the length/diameter of the duct, there will likely exist a shock train instead of a single normal shock. This effective normal shock drops in strength as the gas-generator valve opens because of the reduced expansion seen by the gas as it flows through the gas-generator valve. Generally, total pressure losses are to be avoided. However, this large total pressure drop must be available to enable gas-generator valve control of the solid-fuel gas-generator flow rate that enables ATR throttling. With this large pressure drop, the gas-generator valve can be opened significantly, i.e., throttled down, from the design point before the lower throttle limit is reached. The maximum throttling limit is determined by either gas-generator plenum pressure or the physical size of the minimum gas-generator valve throat area. The minimum physical gas-generator valve throat area is a limit because, as the gas-generator valve is closed down, gas-generator pressure rises. The maximum gas-generator pressure must not exceed the structural limit of the gas-generator case. The maximum potential gas-generator pressure rise will be higher for solid propellants that have a higher burning-rate exponent. Therefore, if significant throttling is required, a solid grain formulation with a lower burning-rate exponent is preferred to minimize gas-generator pressure variations.

### Computer Codes

Several computer codes were required to conduct the research described in this paper. These are described briefly as follows:

Historically, there have been at least two approaches implemented in ATR simulation codes. The first is to specify a fuel/air ratio as well as a compressor operating point (flow rate, pressure ratio, and efficiency). This requires the code to configure a turbine that will drive the compressor, and because of the power balance requirement, provide the specified fuel/air ratio. The turbine configuration includes the number of stages, the maximum tip diameter and throat area, as well as the required inlet pressure. The weakness of this approach is that it can easily generate unfeasible turbine designs. The algorithms used for defining the turbine configuration may be reasonable, but engineering judgment is often required to determine when the range of valid application of the algorithms has been exceeded. This approach requires a realistic and very robust turbine design algorithm.

A second approach, and the one used in the codes developed for this research, assumes that both the turbine and compressor are fully characterized, either on the basis of analysis or test data. This approach does not allow the designer to select the fuel/air ratio, but it does prevent the generation of unfeasible turbine designs. It is most appropriate when a selection of compressors and turbines has already been identified and a comparison of resulting  $I_{sp}$  and specific thrust corresponding to each of the different compressor/turbine combinations is to be accomplished. This approach has been implemented in the development of the most recent ATR codes. The ATR design code creates a data file that characterizes the ATR design (gas-generator throat area, compressor and turbine mass flow rates, speeds, efficiencies and pressure ratios, main combustor throat area, etc.). The ATR off-design code uses this data file to predict off-

design operation and performance of the ATR. Off-design operation is engine operation at other than design conditions. Thus, off-design data include definitions of the flight condition; all engine operating parameters such as temperatures, pressures and mass flow rates; and all performance parameters such as thrust and specific impulse. These off-design data are also stored in a file compatible with the trajectory code used to simulate operation of the ATR in a vehicle.

The DATCOM code is used to predict lift and drag coefficients as a function of Mach and angle of attack for aerodynamic bodies. DATCOM has been used frequently to predict these coefficients for a wide variety of aerospace vehicles. In this research, DATCOM was used to generate a set of aerodynamic coefficients for a generic vehicle. The major emphasis was to consistently use this data set for the vehicle flight simulations, regardless of the propulsion system being used. This approach promotes an unbiased comparison of propulsion systems on the basis of range and flight time, which is the goal of the research.

ZTRAJ is the trajectory analyses code. ZTRAJ is a Fortran code originally developed under the auspices of the Wright-Patterson Laboratory for use on mainframe computers, and was later modified for use on a personal computer. The code is basically batch run and produces output files that can be used to plot both vehicle and engine parameters as they vary during the trajectory.

### Procedure

The general procedure implemented in this research for comparing propulsion systems is outlined here.

The first step was to determine vehicle aerodynamics using DATCOM. The resulting lift and drag coefficients were then put into a data file usable by ZTRAJ. This step may be skipped if the needed aerodynamic coefficients are already available. These coefficients have a tremendous impact on predicted vehicle range and flight time. However, the goal of the research was to generate a valid comparison of propulsion system options. Thus, the consistent use of reasonable aerodynamic data was more important than the actual values of the aerodynamic coefficients used. These same lift and drag coefficients, as a function of angle of attack, were used for all three propulsion systems considered. This is equivalent to using the same vehicle volume and shape for all three propulsion systems. There is an additional drag resulting from the use of inlets for the ATR and turbojet not present with the SRM. However, this additional drag was included in the determination of net thrust for the ATR and turbojet.

The second step was to duplicate the flight performance of a known vehicle/mission. The performance of this vehicle becomes the benchmark against which other propulsion systems are to be compared. Successful completion of this step also provides confidence in subsequent trajectory analyses that use other propulsion systems.

The third step was to define ATR and turbojet designs and analytically fly them in the baseline vehicle.

The last step was to compare the relative performance of the three propulsion systems on the basis of range and time of flight.

### Analysis

The vehicle selected is currently powered by a two-pulse SRM. It has an o.d. of 10 in. with a mass of 800-lbm at launch. Approximate measurements of the fins were done to provide the needed input data for the DATCOM code. The resulting lift and drag coefficients as a function of Mach and angle of attack are shown in Figs. 3 and 4.

The baseline vehicle was flown using a two-pulse SRM. The gross lift off weight (GLOW) for this vehicle was 807 lbm with a usable propellant mass of 340 lbm. The total propulsion system mass (solid motor and propellant) was 400 lbm. This resulted in a burnout mass of 467 lbm. The total inert mass was 407 lbm, which was the same for all three propulsion system options.

The basic mission/flight profile was to first simulate a 3-s ballistic phase. This corresponds to a 3-s drop of the vehicle from the initial flight condition at Mach 0.9 and 10,000 ft altitude. The boost thrust was assumed to be about 2500 lbf, with a sea-level equivalent  $I_{sp}$  of 250 s. The sustained thrust level was assumed to be 1000 lbf, with

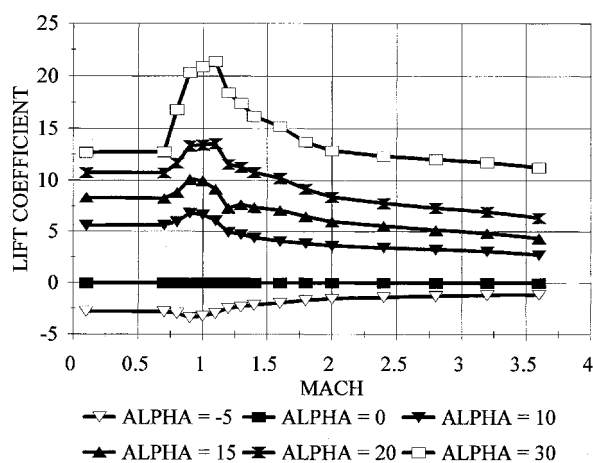


Fig. 3 Lift coefficient vs Mach and angle of attack.

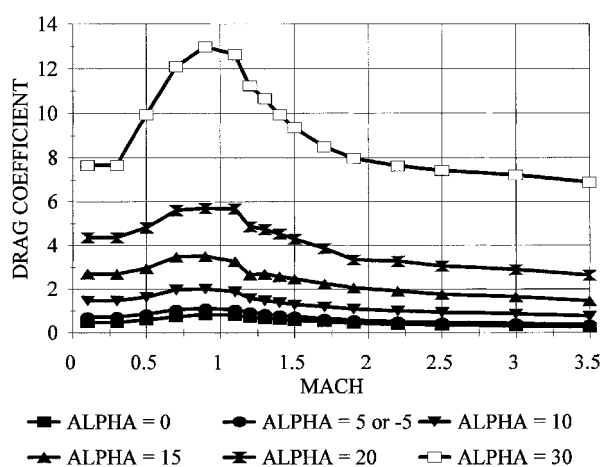


Fig. 4 Drag coefficient vs Mach and angle of attack.

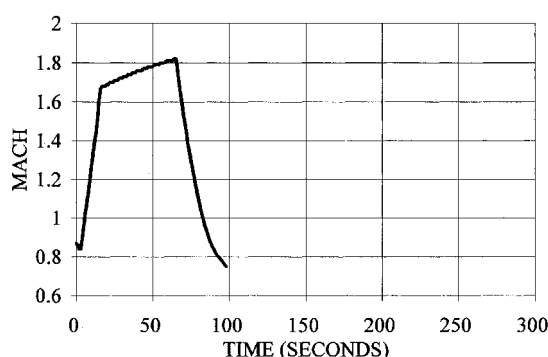


Fig. 5 Mach vs time (SRM-powered vehicle).

a sea-level equivalent  $I_{sp}$  of 235 s. For the given propellant mass, the total burning time of the SRM was 49 s. At SRM burnout, the vehicle had reached the cruise altitude of about 12,000 ft at a Mach number of 1.82 at a range of about 20 miles. The balance of the flight is basically a dive maneuver. The final range was 28.2 miles with a total flight time of 98.1 s. Figures 5 and 6 show Mach and range, respectively, as a function of time during the flight of the SRM-powered vehicle.

Before discussing the results of the ATR-powered vehicle trajectory analyses, some of the more important considerations affecting design of the ATR are noted here.

First, the total volume available for the combination of ATR and propellant is known from the baseline vehicle. This must be allocated between the ATR itself and the solid-fuel gas generator. The

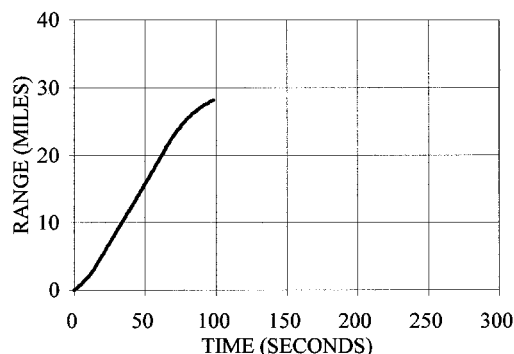


Fig. 6 Range vs time (SRM-powered vehicle).

ATR propulsion-system mass and propellant mass will be different from that of the SRM for at least three reasons: 1) engine mass differences, 2) engine and propellant volume differences, and 3) propellant density differences. Generally, the combined weight of the ATR plus propellant is less than the SRM because the ATR propulsion system does not have as high a propellant volume fraction as that of the SRM. Also, the vehicle normally has a diameter constraint that will limit the burning surface area in an end-burning solid-fuel gas generator. This effectively defines the maximum turbine-drive gas flow rate possible with a reasonable gas-generator pressure.

Some ATR designs may be eliminated because they will not operate over the entire anticipated trajectory. These operational limits include the lower throttling limit described earlier. The compressor also has operation limits that include minimum and maximum speeds as well as the stall limit.

Fuel selection is another consideration. Some fuels can be eliminated for various reasons, including 1) analytically feasible but not adequately developed; 2) excessive soot content in exhaust; 3) metal content in exhaust that can severely degrade turbine performance; 4) burns too hot for use with a turbine; or 5) the molecular weight of the exhaust gas is too high (regardless of how high the heating value may be, the fuel/air ratio will also be high and  $I_{sp}$  will be low).

For the purposes of this study, a relatively high heating value (11,000 Btu/lbm), clean-burning propellant was selected as the ATR fuel.

The turbomachinery performance maps assumed for the ATR were specifically developed for the ATR. The actual design is a monorotor configuration in which the compressor and turbine are mounted back-to-back on the shaft. The wheel diameter (the same for both the compressor and the turbine) is 7.5 in.

The GLOW for the ATR-powered vehicle was 750 lbm, including 93 lbm for the propulsion system. This propulsion system mass included 43 lbm for the ATR and 50 lbm for the gas generator. The usable propellant mass was 250 lbm which resulted in a vehicle burnout mass of 500 lbm. The total inert mass was 407 lbm.

Several ATR engine parameters are important during operation. These include Mach,  $I_{sp}$ , and thrust. These parameters, as they varied during the trajectory, are illustrated, respectively, in Figs. 7 and 8. Figure 9 shows range vs time for the ATR-powered vehicle. It indicates that the ATR-powered vehicle requires a time of flight of 192 s to achieve a range of nearly 50 miles.

The turbojet selected is actually a scaled-up version of a nominal 50-lbf thrust, expendable configuration. It was scaled by a factor of about 12.5 such that the inlet area would match that of the ATR inlet (20 in.<sup>2</sup>). The resulting airflow rates and pressure recoveries, for the same flight conditions experienced in the simulations, were very close to those of the ATR inlet, even though the two codes were developed independently. The GLOW of the turbojet-powered vehicle was 525 lbm, including 54 lbm for the turbojet and 64 lbm for propellant. This resulted in a vehicle burnout mass of 461 lbm. The total inert mass was 407 lbm. Note that the turbojet-powered vehicle GLOW is much less than either the SRM or ATR-powered vehicles. This mass breakdown was determined after initially flying the turbojet-powered vehicle with the available propellant volume completely loaded with JP-10 fuel. The results of this simulation showed

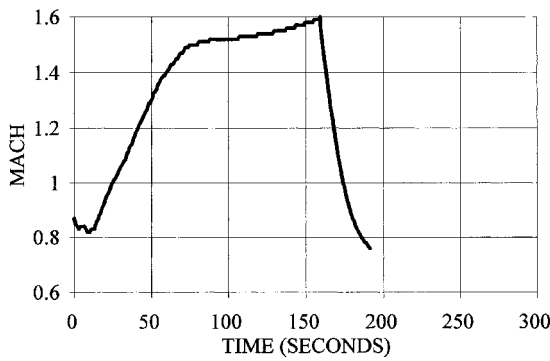


Fig. 7 Mach vs time (ATR-powered vehicle).

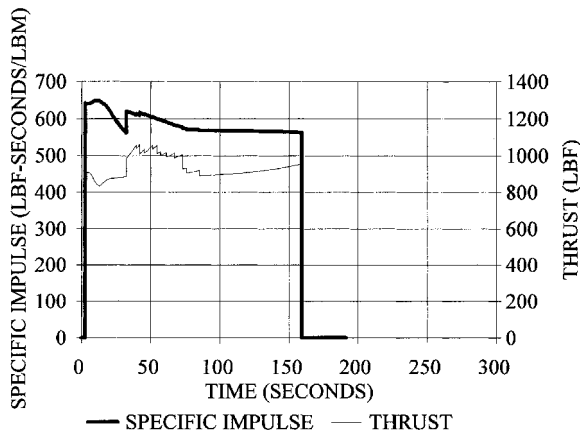


Fig. 8  $I_{sp}$  and thrust vs time (ATR-powered vehicle).

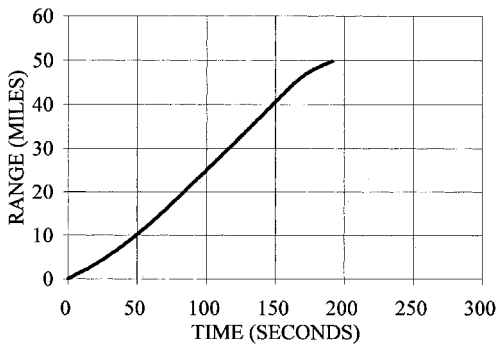


Fig. 9 Range vs time (ATR-powered vehicle).

that 1) the vehicle was unable to achieve supersonic flight; and 2) operating subsonically, the turbojet has a range of over 100 miles with a flight time of nearly 10 min. However, the most important consideration for a vehicle with both range and time-of-flight constraints is the time of flight required to achieve a minimally acceptable range. For comparison with the ATR-powered vehicle in this study, this minimum range is 50 miles. The SRM is unable to make this minimum range because of its low  $I_{sp}$ . The turbojet-powered vehicle achieved a range of 50 miles in ~5 minutes. However, this result for the turbojet is conservative because the vehicle carried a propellant load adequate for a range of 100 miles. For the minimum range of 50 miles, the turbojet-powered vehicle could be significantly shorter and lighter if it were modified to carry only enough propellant to achieve this range. In the analysis, some of the turbojet propellant was off-loaded, as well as some of the inert weight for tankage. The vehicle aerodynamics were unchanged. The off-loading of propellant and the reduction of tankage weight were adjusted until the turbojet-powered vehicle achieved a range of about 50 miles. The result is the much-reduced GLOW used for the turbojet-powered vehicle.

The Mach,  $I_{sp}$ , and thrust for the turbojet-powered vehicle are summarized in Figs. 10 and 11. These figures show that the turbojet-powered vehicle required about 100 s to reach its maximum Mach of 0.9 at the cruise altitude of 12,000 ft.

Although the model simulates supersonic flight operation of a turbojet engine, it does not simulate operation of the latest expendable supersonic turbojet designs. Of particular interest is the specific thrust capability of advanced supersonic turbojet designs. A high specific thrust will be required for missions requiring a short time of flight. However, as with the ATR, if this higher specific thrust comes at the cost of an inadequate mission-average  $I_{sp}$ , a reduced time of flight and/or increased range may not result.

Figure 12 shows range of the turbojet-powered vehicle as a function of time. Flying at a maximum Mach of 0.9, the turbojet-powered vehicle achieved a range of almost 50 miles with a flight time of 290 s.

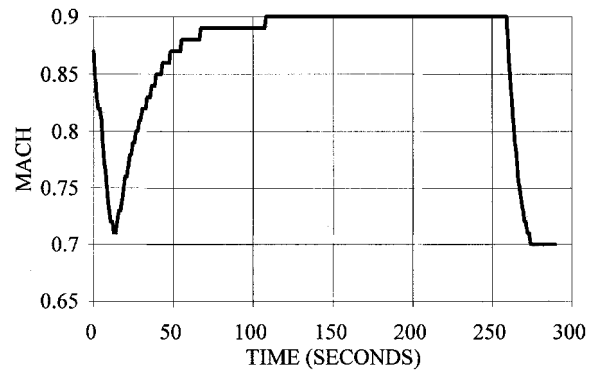


Fig. 10 Mach vs time (turbojet-powered vehicle).

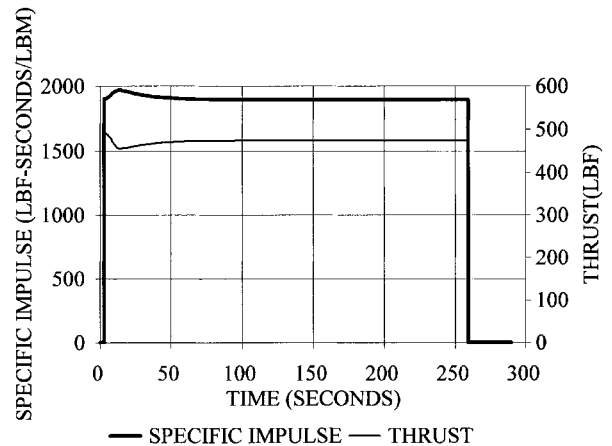


Fig. 11  $I_{sp}$  and thrust vs time (turbojet-powered vehicle).

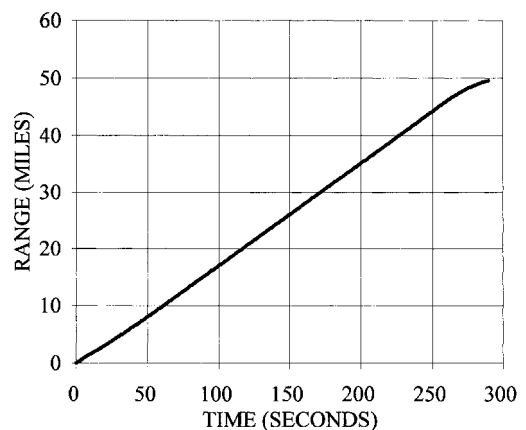


Fig. 12 Range vs time (turbojet-powered vehicle).

Table 1 Propulsion system comparison summary

System	Range, miles	Time of flight, s	Maximum Mach	GLOW, lbm
SRM	28.2	98.1	1.82	807
ATR	49.8	191.5	160	750
Turbojet	49.6	290.0	0.90	525

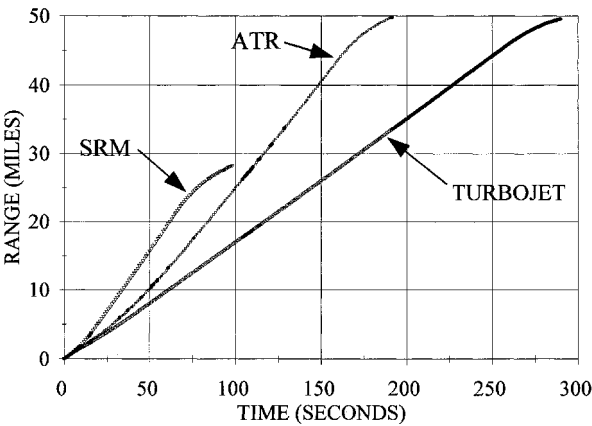


Fig. 13 Range vs time (all propulsion systems).

Results

Figure 13 shows the range and flight time for all three propulsion systems. These same results are also summarized in Table 1. As Table 1 shows, for the same size and shape vehicle, the ATR will provide nearly double the range of an SRM-powered vehicle. The flight time is also roughly double that of the SRM-powered vehicle. This means that the mission average velocity of the ATR is only slightly less than that of the SRM-powered vehicle. Compared with the turbojet-powered vehicle, the ATR achieves the same range in about two-thirds of the time compared to the turbojet. The vehicle mass difference is the penalty paid for the ATR's shorter time of flight.

Further evaluation of the ATR will require consideration of the  $I_{sp}$  and specific thrust capability of the latest expendable super-

sonic turbojet engine designs. In particular, the dependency of  $I_{sp}$  on Mach, which is very pronounced as Mach increases, will have a major effect on both the range and flight time of the supersonic turbojet-powered vehicle.

Conclusions

The use of a solid-fuel gas-generator ATR can reduce the flight time of a turbojet-powered vehicle by about one-third for the same total range. This reduced time of flight is at the expense of a 43% increase in vehicle weight, at least for the vehicle evaluated in this research. A solid-fuel gas-generator ATR-powered vehicle doubles the range and flight time compared with an equal-volume SRM-powered vehicle.

References

<sup>1</sup>Bossard, J. A., Christensen, K. L., and Fedun, M. H., "Return of the Solid Fuel Gas Generator ATR," AIAA Paper 87-1997, July 1987.

<sup>2</sup>Lilley, J. S., Hecht, S. E., Kirkham, B. G., and Eadon, C. A., "Experimental Evaluation of an Air Turbo Ramjet," AIAA Paper 94-3386, June 1994.

<sup>3</sup>Tamaru, T., Shimodaira, K., Saito, T., Yamada, H., and Horiuchi, S., "Hydrogen Fueled Subsonic-Ram-Combustor Model Tests for an Air-Turbo-Ram Engine," *Proceedings of the 9th International Symposium on Air Breathing Engines*, ISABE 89-7028, International Society of Air Breathing Engines, Sept. 1989.

<sup>4</sup>Tanatsugu, N., Naruo, Y., Rokutanda, I., Mizutani, T., Higashino, K., Oguma, M., Kashiwagi, T., and Obata, M., "Results of Sea-Level Static Tests on Air Turbo Ramjet for a Future Space Plane," *Proceedings of the 4th International Space Conference of Pacific Basin Societies, Advances in the Astronautical Sciences*, Vol. 77, American Astronautical Society, Paper 91-640, Nov. 1991.

<sup>5</sup>Tanatsugu, N., Naruo, Y., and Rokutanda, I., "Test Results on Air Turbo Ramjet for a Future Space Plane," AIAA Paper 92-5054, Dec. 1992.

<sup>6</sup>Kashiwagi, T., Obata, M., Ohkita, Y., Tanatsugu, N., and Naruo, Y., "Test Results of the Hydrogen Fueled Model Combustor for the Air Turbo Ramjet Engine," *Proceedings of the 11th International Symposium on Air Breathing Engines*, ISABE 93-7082, International Society of Air Breathing Engines, Sept. 1993.

<sup>7</sup>Christensen, K. L., "Vehicle Performance Optimization Utilizing the Air TurboRamjet (ATR) Propulsion System; Methodology Development and Applications," Ph.D. Dissertation, Dept. of Mechanical and Aerospace Engineering and Engineering Mechanics, Univ. of Missouri-Rolla, Rolla, MO, Dec. 1997.